HHS Public Access

Author manuscript

J Bone Miner Res. Author manuscript; available in PMC 2016 August 02.

Published in final edited form as:

J Bone Miner Res. 2015 November ; 30(11): 2014–2027. doi:10.1002/jbmr.2548.

BMP2 Regulation of CXCL12 Cellular, Temporal, and Spatial Expression is Essential During Fracture Repair

Timothy J Myers[1], **Lara Longobardi**[1], **Helen Willcockson**[1], **Joseph D Temple**[1,2], **Lidia Tagliafierro**[1], **Ping Ye**[1], **Tieshi Li**[1,2], **Alessandra Esposito**[1,2], **Billie M Moats-Staats**[1], and **Anna Spagnoli**[1,2]

[1]Division of Endocrinology, Department of Pediatrics, University of North Carolina at Chapel Hill, Chapel Hill, NC, USA

[2]Department of Pediatrics, Rush University Medical Center, Chicago, IL, USA

Abstract

The cellular and humoral responses that orchestrate fracture healing are still elusive. Here we report that bone morphogenic protein 2 (BMP2)-dependent fracture healing occurs through a tight control of chemokine C-X-C motif-ligand-12 (CXCL12) cellular, spatial, and temporal expression. We found that the fracture repair process elicited an early site-specific response of $CXCL12^{+}$-$BMP2^{+}$ endosteal cells and osteocytes that was not present in unfractured bones and gradually decreased as healing progressed. Absence of a full complement of BMP2 in mesenchyme osteoprogenitors ($BMP2^{cKO/+}$) prevented healing and led to a dysregulated temporal and cellular upregulation of CXCL12 expression associated with a deranged angiogenic response. Healing was rescued when $BMP2^{cKO/+}$ mice were systemically treated with AMD3100, an antagonist of CXCR4 and agonist for CXCR7 both receptors for CXCL12. We further found that mesenchymal stromal cells (MSCs), capable of delivering BMP2 at the endosteal site, restored fracture healing when transplanted into $BMP2^{cKO/+}$ mice by rectifying the CXCL12 expression pattern. Our in vitro studies showed that in isolated endosteal cells, BMP2, while inducing osteoblastic differentiation, stimulated expression of pericyte markers that was coupled with a decrease in CXCL12. Furthermore, in isolated $BMP2^{cKO/cKO}$ endosteal cells, high expression levels of CXCL12 inhibited osteoblastic differentiation that was restored by AMD3100 treatment or coculture with BMP2-expressing MSCs that led to an upregulation of pericyte markers while decreasing platelet endothelial cell adhesion molecule (PECAM). Taken together, our studies show that following fracture, a $CXCL12^{+}$-$BMP2^{+}$ perivascular cell population is recruited along the endosteum, then a timely increase of BMP2 leads to downregulation of CXCL12 that is essential to determine the fate of the $CXCL12^{+}$-$BMP2^{+}$ to osteogenesis while departing their supportive role to angiogenesis. Our findings have far-reaching implications for understanding mechanisms

Address correspondence to: Anna Spagnoli, MD, Department of Pediatrics, Rush University Medical Center 1735 W. Harrison Street 502A Cohn Building Chicago, IL 60612, USA. anna_spagnoli@rush.edu.

Disclosures

All authors state that they have no conflicts of interest.

Authors' roles: Study design, data analysis and interpretation: TJM, LL, HW, LT, TL, AE, PY, JDT, BMM-S, and AS. Study conduct: TJM, LL, HW, and PY. Drafting and revising manuscript: TJM, JDT, LL, HW, and AS. TJM, AS, LL, HW, and PY take full responsibility for data integrity and analysis.

Additional Supporting Information may be found in the online version of this article.

regulating the selective recruitment of distinct cells into the repairing niches and the development of novel pharmacological (by targeting BMP2/CXCL12) and cellular (MSCs, endosteal cells) interventions to promote fracture healing.

Keywords

BMP2; CXCL12; FRACTURE REPAIR; ENDOSTEAL CELLS; MESENCHYMAL STROMAL CELLS

Introduction

Bone is generally perceived as a highly regenerative tissue; however, there are clinical conditions in which the healing can either fail (non-unions), or its course should be accelerated (osteoporotic fractures). Increased longevity has increased the prevalence of osteoporosis, leading, in the United States, to over 1.5 million osteoporotic annual fractures, expected to double by 2025 with related expenditures of $25.3 billion/year.[1] In osteoporotic fractures, morbidity and mortality increase proportionally with the length of healing. Accelerating or facilitating the fracture healing will lead to improvement in patient care, especially in the elderly population. Ten percent of fractures fail to heal, leading to non-unions. Approximately 600,000 people in the United States suffer from non-unions, and the total health cost is about $14.6 million/year.[2–5] Treatments for non-unions are limited. Despite its clinical significance, mechanisms governing the temporal and spatial orchestration of cellular and humoral responses during fracture repair are still unknown. Revealing these mechanisms may identify therapeutic targets to promote healing.

Expression of bone morphogenic protein 2 (BMP2) in fracture repair is biphasic; within the first 24 hours the highest level of BMP2 expression is registered, whereas later expression occurs during the hard callus formation phase.[6] Initiation of fracture healing fails to occur when BMP2 is conditionally knocked-out in osteochondroprogenitors,[7] showing that BMP2 is required early in fracture repair, though the mechanism of action remains unknown. In humans, there is a reduction in BMP2 expression within areas of non-unions compared to healing fractures.[8,9] Here, we report that BMP2 exerts its fracture regenerative effects by controlling endosteal CXCL12 temporal and cellular expression and commitment to osteogenesis.

Upregulation of CXCL12 expression is found in human and mouse sera within the first 2 days after bone defects.[10,11] CXCL12 is considered a master regulator of cell mobilization, including mesenchymal stromal cells (MSCs) and in bone injury models.[12–15] More recently, CXCL12 has been reported to play a role in stem cell behavior by regulating maintenance, survival, and differentiation of hematopoietic stem cells (HSCs)[16] and possibly osteogenic precursors, including MSCs.[17–19] In vitro studies have shown that BMP-dependent osteogenic differentiation is regulated by CXCL12.[12,20–22]

In this study, we analyzed the mechanism by which BMP2 induces fracture healing, and in particular the interplay between BMP2 and CXCL12 in the commitment of endosteal cells to an osteoblastic lineage. We found that BMP2-dependent fracture healing occurs through

temporal and spatial regulation of CXCL12 expression in endosteal cells. BMP2 downregulates CXCL12 and CXCL12-supporting factors in endosteal cells, and BMP2 regulation of CXCL12 expression both in vivo and in vitro leads to osteoblastic differentiation and fracture healing. Furthermore, we showed that MSC transplant can be a means to deliver BMP2 at the fracture site, and manipulation of CXCL12 signaling can restore healing in the absence of a full complement of BMP2. Our studies provide evidence that in fracture repair, osteoblastic differentiation and CXCL12 expression are closely related and are tightly regulated by BMP2. Further, the downregulation of CXCL12 can be a key switch for endosteal cells from an endothelial-supporting function to osteoblastic commitment.

Materials and Methods

Antibodies and reagents

Primary antibodies used were as follows: anti-SDF-1(CXCL12; #sc-28876; Santa Cruz Biotechnology, Santa Cruz, CA, USA) or anti-SDF-1 (CXCL12; #11353; Biorbyt, San Francisco, CA, USA); rat anti-CD31 (platelet endothelial cell adhesion molecule [PECAM]; #ab56299; Abcam, Cambridge, UK); mouse anti-NG2 (#MAB5364; Millipore, Billerica, MA, USA); anti-α-SMA (#ab21027; Abcam); anti-phospho-Smad1/5/8 (#9511; Cell Signaling Technology, Beverly, MA, USA); anti-mouse CXCR4 (clone 247506; R&D Systems, Minneapolis, MN, USA); anti-mouse osteocalcin (Clone R21C-01A; TaKaRa Bio-Clontech, Mountain View, CA, USA). Secondary antibodies used were as follows: donkey anti-rabbit IgG conjugated to Cy3; donkey anti-rat IgG conjugated to Alexa Fluor 488, and Fab Fragment donkey anti-mouse conjugated to Alexa Fluor 647 Cy5 (all from Jackson ImmunoResearch, West Grove, PA, USA). Recombinant BMP2 was purchased from R&D Systems. The inhibitor AMD3100 was from Selleck Chemicals, whereas the collagenase and trypsin were from Sigma (St. Louis, MO, USA).

Animal models

$BMP2^{flox/flox}$ mice were kindly provided by Dr. James Martin (Texas A&M Health Science Center)[23]; mice were originally on a mixed C57B/L6 background and were crossed for more than four generations in C57B/L6 background. To generate $BMP2^{cKO/+}$mice, $BMP2^{flox/flox}$ mice were crossed with Prx1 limb enhancer driven-Cre transgenic males (C57B/L6 background) (C. Tabin, Harvard Medical School), which drives Cre-expression in osteochondroprogenitors.[24] $BMP2^{cKO/+}$ mice, which had no obvious phenotype because they were similarly sized, healthy, fertile, and aged normally compared to controls (Supporting Fig. 1B, C), were crossed with $BMP2^{flox/flox}$ to produce $BMP2^{cKO/cKO}$. In almost all experiments, Cre-negative sibling mice, regardless of flox status, were used as controls. Genotyping was done by PCR analysis for BMP2 floxed alleles and Cre expression using the following primers: $BMP2^{flox}$ For (5′-aagtctcctccttcatcagtatacgctcg-3′); $BMP2^{flox}$ Rev (5′-ccacacagagtcaaggtttaaaaggatgc-3′); Cre For (5′-tccaatttactgaccgtaacaccaa-3′); Cre Rev (5′-cctgatcctggcaatttcggcta-3′) (Supporting Fig. 1A). We verified that BMP2 expression was decreased (more than 90%) respectively in MSCs (Supporting Fig. 1B) and endosteal cells (Supporting Fig. 5A) from $BMP2^{cKO/cKO}$ and in MSCs from $BMP2^{+/cKO}$ (almost 60%) mice (Supporting Fig. 1B). BMP2-LacZ reporter mice on an FVB/NJ background were

genetically modified using bacterial artificial chromosome system to produce β-gal expression under control of the BMP2 promoter and enhancer region were provided by D.G. Mortlock (Vanderbilt University).[25]

Tibia fracture model

Animal studies were approved by the Institutional Animal Care and Use Committee of the University of North Carolina (Chapel Hill, NC, USA). Stabilized tibia fractures were produced in C57B/L6 background or FVB/NJ female mice between 9 and 12 weeks of age as described.[26] For treatment with AMD3100, mice were i.p.-injected with 2.5 μg/g AMD3100-PBS solution twice per day 2 days once prior to fracture and then six times beginning 2 days after fracture (day 2 through day 7) followed by harvest at 14 days postfracture.

Micro–computed tomography analysis of fracture calluses

Fractured tibias were dissected 14 days postfracture, fixed in 4% paraformaldehyde in PBS for 18 hours at 4°C, rinsed, and scanned by micro–computed tomography (μCT) (Scanco Medical μCT 40) housed in the UNC Biomedical Research Imaging Center. μCT images were obtained at 55 kVp, 145 μA, 300 ms integration time using 12-μm voxel resolution along a length of the tibia centered on the fracture line. Three-dimensional reconstruction and colorimetric images were done using Analyze 9 software (AnalyzeDirect, Stilwell, KS, USA). Volumetric analysis of tissue composition was measured only in the callus by narrowing the analysis from the first proximal (top) to the last distal (bottom) sign (indicated by periosteal enlargement) of the callus formation when examining the coronal plane of the μCT images as reported.[26,27] Further narrowing to within the fracture line was done by including only areas with signs of breaking within the cortical bone in the transversal plane, as reported.[26,27] Tissue volume was determined by quantifying the positive voxels within a threshold range for soft tissue, new bone, and cortical bone based on a parametric thresholding study combining serial μCT scanning and histological analysis as described.[26,28] Results presented are volumes of each threshold range divided by the number of slices encompassing the callus to normalize for varying callus size.

Histology, immunohistochemistry, immunofluorescence, and in situ hybridization studies

Tibias from at least two individual animals per group were dissected at 3, 7, 10, 14, and 21 days postfracture and subjected to either immunohistochemistry (IHC), immunofluorescence (IF), or in situ hybridization (ISH). For IHC, tibias were fixed in 4% paraformaldehyde for 18 hours, then decalcified in 10% EDTA solution for 2 weeks, embedded in paraffin, and the entire callus was sectioned at 6 μm in either the longitudinal or axial plane and adhered to microscope slides coated with Biobond (Electron Microscopy Science, Hatfield, PA, USA). For IF, tibias were fixed in 4% paraformaldehyde for 18 hours, then decalcified in RapidCal Immuno (BBC Chemical, Mount Vernon, WA, USA) for 3 days before soaking in 30% sucrose for approximately 48 hours. Tissue was embedded in OCT and sectioned on a cryostat at 7 to 8 μm. The center of the fracture gap was identified as the largest diameter of the callus in which the fracture line was clearly seen following a serial hematoxylin and eosin staining. All further histological analyses were performed within 500 μm of the center of the fracture line. For IHC, Vectastain ABC kit (Vector Laboratories, Burlingame, CA,

USA) was used according to the manufacturer's instructions. Briefly, sections were incubated in 3% H_2O_2 diluted with 0.01 M PBS for 10 min, blocked for 1 hour with appropriate serum, and incubated in primary antibody (diluted in blocking solution) overnight at room temperature. Sections were incubated in the appropriate biotinylated secondary antibody diluted in blocking buffer for 1 hour. Sections were then incubated in Avidin-Biotin complex and then visualized with diaminobenzidine. As a control, sections were processed with the omission of primary antibodies which completely abolished specific staining. ISH analysis was performed as described.[29] Plasmids carrying the cDNA insertions for mouse *Collagen I* (*ColI*), *Osterix* (*Osx*), and *Osteocalcin* (*Ocn*) were kindly provided by G. Karsenty (Columbia University), the probe for *Collagen-X-α-1* was provided by D.G. Mortlock (Vanderbilt University), the probe for *Cxcl12* was generously donated by Matthew J. Hilton (Duke University). *β-galactosidase* staining was performed as described.[25] In short, extracted tibias were briefly fixed in 0.4% paraformaldehyde for 30 minutes at 4°C. Following washing in PBS, the whole bone was incubated in staining solution overnight at room temperature. The tissue was further fixed in 4% paraformaldehyde at 4°C for 18 hours and treated for paraffin embedding as described above for IHC. Images were taken with an Olympus BX51 microscope and a DP71 camera. For IF, sections were pretreated for autofluorescence with 1% $NaBH_4$ for 20 minutes, blocked for endogenous mouse IgG (Jackson ImmunoResearch) combined with 5% NDS (0.1 M PBS with 0.01% Triton X) for 1 hour and incubated in primary antibodies for SDF1, PECAM, and NG2 in 2% NDS buffer overnight at room temperature. Primary antibodies used were as follows: rabbit anti-SDF-1 (#11353; Biorbyt); rat anti-CD31; mouse anti-NG2 (#MAB5364; Millipore). Sections were incubated in the appropriate secondary antibody (donkey anti-rabbit IgG conjugated to Cy3; donkey anti-rat IgG conjugated to Alexa Fluor 488, and Fab Fragment donkey anti-mouse conjugated to Alexa Fluor 647 Cy5 (Jackson ImmunoResearch) diluted in 2% NDS buffer for 2 hours. Sections were imaged on an Olympus FV1000 MPE SIM Laser Scanning Confocal Microscope with a 60× PlanApo oil immersion lens zoomed 2× using sequential scanning. Images were viewed with Olympus FV10-ASW Viewer software and final images were merged with Image J.

Endosteal cell isolation

For in vitro experiments, endosteal cells were isolated from the bone marrow of tibias and femurs using the procedure of Balduino and colleagues.[30,31] Briefly, tibias and femurs were dissected and all extraneous tissue removed and then treated with five incubations for 30 min in 0.1% collagenase and 0.125% trypsin in Hank's balanced salt solution. The bone marrow was removed by flushing with MSC culture medium and saved and cultured as described below (Isolation and expansion of primary MSCs). Following washing, bones were broken into segments and treated twice with 0.1% collagenase for 40 min at 37°C. Each fraction was stopped and washed with Dulbecco's modified Eagle's medium with antibiotics and 10% fetal bovine serum (maintenance media) (Atlanta Biologicals, Norcross, GA, USA) before being seeding onto tissue culture dishes and allowed to expand to confluence. The first treatment contains subendosteal and endosteal cells and the second treatment contains endosteal osteoblasts. Cells were grown at 37°C and 5% CO_2 for three passages before being using for experiments. Osteoblastic differentiation was carried out using StemXVivo osteogenic base media plus 0.5× Stem XVivo osteogenic supplement

(R&D Systems). Media was changed every 3 days for the length of the experiment. Where indicated, 100 ng/mL recombinant human BMP2 was added to cells beginning at day 0 and freshly supplemented when changing media. Mineralization was determined by staining with a 2% solution of Alizarin red for 15 min following fixation in formalin. For in vitro AMD3100 treatment of confluent endosteal cells, osteogenic differentiation was again initiated with StemXVivo media and supplement. Beginning on day 7, 400 μM of AMD3100 dissolved in water was added to the cells every 3 days until day 14 when cells were harvested.

RNA isolation and qRT-PCR

When indicated, cells were harvested using μMACS mRNA Isolation kit (Miltenyi Biotec, San Diego, CA, USA). Contaminating DNA was removed with DNase I (New England BioLabs, Ipswich, MA, USA) and extracted mRNA was converted to cDNA using μMACS One-Step cDNA Kit (Miltenyi Biotec). To determine the expression of marker genes, we performed qRT-PCR using 2× Sso Advanced SYBR Green supermix and a CFX96 Connect Real-Time System and CFX Manager software (Bio-Rad Laboratories, Hercules, CA, USA). Analysis of relative gene expression was made using the Pfaffl method with both mouse β-actin and GAPDH as housekeeping genes. Primers are reported in Supporting Table 1.

Isolation and expansion of primary MSCs

Primary cultures of BM-derived MSCs were obtained by flushing the BM from the long bones of 4-week-old to 6-week-old male littermates as reported.[29] Briefly, BM-nucleated cells were cultured for 8 to 10 days without passaging to allow selection by plastic adherence. Cells were separated from contaminating hematopoietic cells through immunodepletion of CD45, CD11b, CD34-positive cells using the MACS system (Miltenyi Biotech). As described, and verified during the presently reported studies, after immunodepletion, CD45, CD11b, were less than 3.0%[26] and CD34 were 2.3% ± 1.6%, $n = 3$. Immediately following immunodepletion, 1×10^6 MSCs in 200 μL sterile normal saline were systemically transplanted by tail vein injection into randomly selected $BMP2^{cKO/+}$ fractured mice.

Coculture with primary MSCs

MSCs from control or $BMP2^{cKO/cKO}$ mice were obtained as described above (Isolation and expansion of primary MSCs). $BMP2^{cKO/cKO}$ endosteal cells and MSCs were plated at the same time in a 10:1 ratio of endosteal:MSCs and allowed to plate down overnight. The following day, osteogenic differentiation was initiated. Media was changed every 3 days until RNA was harvested at day 14.

Biomechanical testing

After μCT analysis, 14-day postfracture samples were subjected to distraction-to-failure tension Biomechanical testing (BMT). As reported, the bone ends were potted with polymethylmethacrylate and loaded into the Electroforce system ELF 3200 (Bose Corporation, Framingham, MA, USA).[26] The displacement rate was set at 0.25 mm/min

and a force displacement curve recorded to calculate the ultimate force (maximum force at failure) and stiffness (maximum slope) using WinTest Control software.

Statistical analysis

Data are expressed as mean ± SE. For cell culture, each experiment included three samples. Statistical analyses were performed using a two-tailed unpaired Student's *t* test for two comparisons or one-way ANOVA followed by Sidak's test for multiple comparisons by Prism 6 (GraphPad Software, Inc., La Jolla, CA, USA). Statistical significance was set at $p \leq 0.05$.

Results

CXCL12 expression in response to fracture

We found that in the bones juxtaposing the fracture line, CXCL12 is expressed by endosteal cells and a few layers of osteocytes underneath the endosteum as early as day 7 and day 14 postfracture (Fig. 1*A*: A2, A3, A5, A6). This endosteal CXCL12 cellular response is fracture-induced; as in unfractured control and $BMP2^{cKO/cKO}$ mice, CXCL12 expression is primarily seen within the BM (Fig. 1*A*: A1, A4, A7, and A10). Interestingly, the CXCL12 endosteal response preceded a faint CXCL12 periosteal expression that was only notable 14 days after fracture (Fig. 1*A*: A3). In $BMP2^{cKO/+}$ (Fig. 1*A*: A8, A9, A11, and A12) and $BMP2^{cKO/cKO}$ (Supporting Fig. 2) mice, CXCL12 is expressed by endosteal cells and osteocytes, but the expression is increased, has a disorganized pattern and is clustered in vascular-like formations. Whereas after fracture the CXCL12 expression at the periosteal site appeared to be normal in $BMP2^{cKO/+}$ (Fig. 1*A*: A8, A9, A11, and A12) as well as in $BMP2^{cKO/cKO}$ mice. Because $BMP2^{cKO/cKO}$ mice have spontaneous fractures[7] that would confound results and short and bent tibias that would make intramedullary fixation difficult, we decided to use the $BMP2^{cKO/+}$ mice for further experiments (Supporting Fig. 1C). As indicated by μCT analyses, $BMP2^{cKO/+}$ shows a small callus, compared to control, reminiscent of an atrophic non-union fracture (Fig. 1*C–F*). We also assessed the CXCL12 mRNA expression pattern by ISH and found that it was similar to the protein expression pattern assessed by IHC (Supporting Fig. 3).

To investigate whether the deranged CXCL12 expression in $BMP2^{cKO/+}$ mice had a functional role, we evaluated whether the blockage of CXCL12 signaling in $BMP2^{cKO/+}$ mice could restore the callus properties. We treated $BMP2^{cKO/+}$ mice with AMD3100, an antagonist for CXCR4 and agonist for CXCR7, and then subjected 14-day postfracture tibia samples to μCT scanning and quantification of total callus, new bone, and soft tissue volumes using previously reported volumetric parameters.[26,27] Based on the finding that the CXCL12 endosteal response occurred early on during the fracture repair process, we administered AMD3100 once 2 days prior to fracture and then beginning 2 days after fracture to 7 days after fracture. CXCL12 AMD3100 treatment restored callus formation in $BMP2^{cKO/+}$ mice (Fig. 1*B*). Analyses of the callus components showed that within the total callus AMD3100 treatment increased the soft cartilaginous tissue (Fig. 1*B–E*). We also noted that AMD3100 in $BMP2^{cKO/+}$ induced new bone formation at the fracture line at a level that was similar to controls (Fig. 1*E*). Histological Safranin O/Fast Green staining and

ISH analyses confirmed a decrease in the callus size of $BMP2^{cKO/+}$ fractures, as well as a decrease in hypertrophic chondrocytes (ColX) and pre-osteoblasts and mature osteoblasts (osterix and osteocalcin). AMD3100 treatment was able to induce a callus with cartilaginous and newly formed bone tissue corroborating the μCT quantitative analyses (Fig. 1*F*). AMD3100 treatment did not significantly affect control fractures (Fig. 1*B*–*F*). Although a trend for soft tissue increase was noted, this was also nonstatistically significant. Taken together, results indicate that proper BMP2-dependent regulation of CXCL12 within the injured tissue is critical for fracture healing to occur.

BMP2 regulation of CXCL12

We next evaluated the time-course for the CXCL12 cellular response during healing and its BMP2-dependent regulation. In control fractures, CXCL12 endosteal expression decreased in a time-dependent manner beginning at day 14 through day 21 (Fig. 2*A*). We also noted a spatial regulation of CXCL12 expressing osteocytes within the cortical bone, that at day 7 were localized beneath the endosteum and by day 14 were found to be in deeper sheets of the cortical bone. IHC for osteocalcin (on adjacent sections) and morphology indicated that CXCL12 cortical bone expressing cells were osteocytes (Supporting Fig. 4). In the $BMP2^{cKO/+}$ fractures, high levels and disorganized expression of CXCL12 remained in the endosteum and osteocytes at day 14 throughout day 21 (Fig. 2*A*). We also noted that CXCL12 expression in $BMP2^{cKO/+}$ was associated with vascular-like formations that were confirmed to be endothelial cells as indicated by the positive immunostaining for PECAM (Fig. 2*B*). We then further investigated the nature of the vascular-like formations that were particularly abundant in $BMP2^{cKO/+}$ mice and the relationship with CXCL12 expression. We found that in $BMP2^{cKO/+}$, CXCL12-expressing cells are localized around the increased PECAM-expressing vascular formations and most of the $CXCL12^{+}$ cells coexpressed the pericyte marker α-SMA and the marker NG2 (Fig. 2*C*, *D*). Notably, the major producer of CXCL12 within the BM and specifically within the endosteal niche is considered to be CXCL12-abundant reticular (CAR) cells, which are perivascular.[32] There is evidence that CAR cells are a population of pericyte cells that could regulate vascular endothelial cells while also possibly being osteoprogenitor cells.[17–19,32] To further evaluate the BMP2-CXCL12 interplay, we isolated endosteal cells from control and $BMP2^{cKO/cKO}$ hind-limb long bones and found that in the absence of BMP2 expression, CXCL12 expression is higher than in controls (Fig. 2*E*). We also noted that in the absence of BMP2, there is an increase of PECAM in endosteal cultures (Fig. 2*F*), reflecting more endothelial cells in the culture and consistent with the aberrant angiogenesis found in $BMP2^{cKO}$. We found no statistical difference in CXCR4 and CXCR7 mRNA expressions in $BMP2^{cKO/cKO}$ endosteal cells compared to control.

To determine the cellular expression of BMP2 and CXCL12 over the healing time course, we used a BMP2-LacZ reporter mouse.[25] We observed BMP2 expression at day 3 in the BM and along the endosteum, which persisted through day 10 but was gone by day 14 (Fig. 2*G*). When comparing CXCL12 expression to BMP2 expression, nearly all BMP2 expressing endosteal cells also expressed CXCL12 and the CXCL12 receptor CXCR4 (Fig. 2*G*, *H*), indicating that the CXCL12–fracture-induced response is indeed a $BMP2^{+}$/$CXCL12^{+}$ endosteal cellular response. BMP2-LacZ reporter expression was confirmed by

the fact that all LacZ-positive cells were also positive for phospho-SMAD-1,5,8 (Fig. 2*H*). Interestingly, at a later stage of fracture repair (14 days), we found BMP2 expressing cells within the callus (resembling hypertrophic chondrocytes), but those cells did not express CXCL12 (Fig. 2*G*, indicated by an arrow).

We next analyzed the direct effect of BMP2 on CXCL12 in cultured endosteal cells under osteogenic conditions. Treatment of endosteal cells with BMP2 led to a decrease in CXCL12 mRNA expression during osteogenic differentiation (Fig. 3*A*). Hepatocyte growth factor (HGF), which is reported to increase expression of CXCR4, and CD164, which can act as a coreceptor for CXCL12 with CXCR4, also decreased in response to BMP2 (Fig. 3*B*). [33,34] Decreasing CXCL12 was coupled with down-regulation of PECAM (Fig. 3*C*). Expression of osteogenic markers and mineralization, as seen by Alizarin red (AR) staining, confirmed BMP2-induced osteogenic differentiation (Fig. 3*D*). BMP2 also induced increases in the pericyte markers α-SMA, NG2, and PDGFRβ (Fig. 3*E*) while downregulating CXCL12-related niche genes, stem cell factor (SCF), and angiopoietin-1 (Ang-1) (Fig. 3*F*); however, BMP2 had no effect on CXCR4 and CXCR7 expressions.

We then evaluated the osteogenic capabilities of endosteal cells in the absence of endogenous BMP2 by using $BMP2^{cKO/cKO}$ cells. In control cells there is an increase in osteogenic markers RunX2, osterix, and osteocalcin over time (Fig. 4*A*) that correlated with increased mineralization by AR staining (Fig. 4*B*). In these cells, the CXCL12 expression pattern shows an initial increase during the first 7 days of differentiation, with a decrease by 14 days (Fig. 4*C*). Lack of BMP2 in $BMP2^{cKO/cKO}$ endosteal cells impairs osteoblastic differentiation (Fig. 4*A*, *B*) and CXCL12 expression remains steady at early stages and increases dramatically between 7 and 14 days (Fig. 4*C*). To determine a functional role for CXCL12 signaling, we treated $BMP2^{cKO/cKO}$ endosteal cells with AMD3100 beginning at day 7. AMD3100 treatment led to $BMP2^{cKO/cKO}$ endosteal cell differentiation as determined by increases in RunX2, osterix, and osteocalcin after 14 days (Fig. 4*D*), decrease of PECAM expression (Fig. 4*E*), and increases in expression of pericyte markers (Fig. 4*F*), which were no different than control in non-differentiating conditions (Supporting Fig. 5B). Treatment of control cells with AMD3100 had no effects on Runx2, Osterix, PECAM, α-SMA, NG2, and PDGFRβ (Supporting Fig. 6). Interestingly, AMD3100 had no effect on CXCR7 but decreased CXCR4 expression (21% ± 3% of control; $p < 0.001$), indicating that AMD3100 effects may also be mediated by a decrease on CXCR4 expression. Together these data suggest that CXCL12 is a requirement for proper osteogenic differentiation of endosteal cells while leading away from an endothelial-supporting function.

MSC-derived BMP2 regulates CXCL12 expression

We have previously showed that systemically transplanted MSCs migrate and can home to the injury site where they express BMP2 and enhance fracture healing through paracrine effects.[26] To study the functional paracrine effect of MSC-derived BMP2 on CXCL12 and fracture healing, we tested whether CXCL12 regulation could be restored by transplanting wild-type MSCs into fractured $BMP2^{cKO/+}$ mice. We traced our transplanted MSCs using cells from BMP2-LacZ reporter mice and found that MSCs localized to the endosteum where they expressed both BMP2 and CXCL12 (Fig. 5*A*). By day 7 and sustained at day 14,

MSC-transplanted mice had lower levels of endosteal CXCL12 compared to $BMP2^{cKO/+}$ mice and better organized pattern of expression within the cortical bone (Fig. 5*B*), showing that MSC transplant is able to rescue CXCL12 regulation.

We next determined whether MSC-dependent regulation of CXCL12 restored fracture healing in $BMP2^{cKO/+}$ mice. By μCT analyses we observed that in $BMP2^{cKO/+}$ mice transplanted with MSCs, total callus, soft tissue and new bone volumes were restored to control levels (Fig. 5*C*). Safranin O/Fast Green and ISH analyses revealed that in $BMP2^{cKO/+}$ which received MSCs, callus formation was restored, as indicated by osterix expression at day 7 and osteocalcin and collagen I at day 14 (Fig. 5*D*). Biomechanical testing at day 14 by both distraction-to-failure (Fig. 5*E*) and three-point bending (Supporting Fig. 7A, B) showed that in $BMP2^{cKO/+}$, MSC transplant restored biomechanical properties.

The restoration of new bone in $BMP2^{cKO/+}$and the ability of BMP2 to induce endosteal osteogenic differentiation led us to evaluate whether MSC-derived BMP2 could directly regulate CXCL12 expression in endosteal cells. To assess the role of MSC-derived BMP2 on endosteal differentiation, we attempted to use conditioned media and transwell experiments to induce endosteal differentiation; however, we did not detect any signs of osteogenic differentiation in these conditions (data not shown). We then performed direct contact experiments with fluorescently labeled endosteal cells cocultured with MSCs where shRNA was used to knockdown BMP2 expression in MSCs (Supporting Fig. 8A). FACS was used to separate the population of labeled endosteal cells from MSCs following 21 days of osteogenic differentiation. MSCs carrying a control shRNA induced a significant reduction of endosteal cell-CXCL12 HGF, CD164, and SCF (Supporting Fig. 8A–D), whereas MSCs lacking BMP2 induced a significantly higher expression of CXCL12 and other genes. To have a more robust knockdown, we used $BMP2^{cKO/cKO}$ endosteal cells in a coculture model with MSC from control and $BMP2^{cKO/cKO}$ mice. MSCs from control mice induced a downregulation of CXCL12 and CXCL12-supporting genes along with a decrease of PECAM expression after 14 days of culture (Fig. 6*A*, *B*). This correlated with an increase in osteoblastic markers, along with pericyte markers αSMA, NG2, and PDGFRβ, whereas SCF and Ang-1 decreased (Fig. 6*C*–*E*). Regulation of CXCL12, CXCL12-supporting genes, PECAM, αSMA, NG2, and PDGFRβ, SCF, and Ang-1 was either abolished, or even paradoxically, enhanced when endosteal cells were cocultured with MSC from $BMP2^{cKO/cKO}$ mice (Fig. 6*A*–*E*). Our results show that MSC-derived BMP2 can restore appropriate CXCL12 expression leading to osteogenic differentiation of endosteal cells.

Discussion

BMP2 is a critically important component of the fracture healing process but its mechanism of action is still unknown. Here we report that a BMP2-dependent temporal, spatial, and cellular regulation of CXCL12 is essential for the fracture repair process to initiate. We found that the fracture healing impairment found in the absence of a full complement of BMP2 leads to CXCL12 temporal and expression pattern derangement. By either controlling the CXCL12 signaling or by transplanting MSCs expressing BMP2 there was a return of proper healing and CXCL12 expression patterns in BMP2-haploinsufficient mice. Our in situ and in vitro studies showed that we have identified a population of $CXCL12^{+}$-$BMP2^{+}$

endosteal cells that are induced by the fracture-injury process. Furthermore, we have defined that BMP2 has a functional role in the timing of CXCL12 expression and determining the fate of the $CXCL12^{+}$-$BMP2^{+}$ endosteal cell population. To summarize the findings, a model is presented in Fig. 7, in which, following fracture, a $CXCL12^{+}$-$BMP2^{+}$ endosteal-perivascular cell population is recruited along the endosteum, then a timely increase of BMP2 leads to downregulation of CXCL12 that is essential to determine the fate of the perivascular cells into pericytes-osteoblasts-osteocytes that eventually integrate into the newly forming bones (Fig. 7). In the absence of BMP2, such tight regulation of CXCL12 is lost and the $CXCL12^{+}$-$BMP2^{-}$ endosteal-perivascular cells become committed to their endothelial-supportive role leading to abnormal angiogenesis, deranged osteocyte organization, and healing impairment.

The identification and characterization of the functional role of mesenchyme progenitors in maintaining the BM homeostasis and their presumptive localization at the interface between the BM and bone have been the object of several recent studies, some focusing on the identification of CXCL12-expressing cells. Omatsu and colleagues[35] showed that CXCL12 perivascular-expressing cells were necessary for HSC homeostasis and may serve as osteo-adipocyte-progenitors. Mendez-Ferrer and colleagues[19] showed that $Nestin^{+}$-$CD45^{-}$ cells express CXCL12 and contribute to bone and growth plate cartilage. Greenbaum and colleagues[18] showed that PRX1+CXCL12+ support selective aspects of hematopoiesis. Little is known about the in vivo functional role of mesenchyme progenitors in response to fracture.[36,37] Here, we report the identification and the in vivo functional role of a $CXCL12^{+}$-$BMP2^{+}$ endosteal-perivascular cell population to initiate the fracture repair process. There is some evidence for the action of CXCL12 on the skeletal system in inducing chondrocyte hypertrophy and BMP-dependent osteoblastic differentiation of progenitors,[23,33,34] as well as cell recruitment in bone injuries.[38,39] An appropriate control of CXCL12 expression appears critical, in fact, long-term continuous treatment before fracture or load-induced bone formation can inhibit bone production.[40,41] We identified the temporally regulated expression pattern of CXCL12 and showed that it is initially induced by the fracture event and then decreases with the progression of the repair process. Therefore, we designed our in vivo and in vitro rescue experiments to allow for an initial phase of CXCL12 signaling followed by AMD3100 treatment when CXCL12 expression would decrease. We found that AMD3100 induced callus formation in BMP2-insufficient mice. Likewise, AMD3100 treatment of BMP2-deficient endosteal cells was able to restore osteoblastic differentiation. Interestingly, we found a faint CXCL12 expression at the periosteal site but only 14 days after fracture, whereas the endosteal response was as early as 3 days after fracture and this response was not altered in BMP2 mutants. Furthermore, although CXCL12 endosteal cells coexpress BMP2, CXCL12 periosteal cells did not express BMP2. Our studies do not dispute that periosteal-derived cells are critical during the fracture repair; rather they provide novel evidence to support previous findings indicating that endosteal cells contributed to the early stage of the repair process and were critical to the formation of the intramembranous callus.[42–45] Although we cannot exclude that a periosteal loss of BMP2 may contribute to the fracture repair failure found in $BMP2^{cKO/+}$, it is unlikely that this would impact the role of CXCl12 in periosteum-derived healing. In fact, we provide strong evidence that the CXCL12 endosteal

response occurred before the periosteal response and the endosteal response but not the periosteal was deranged in $BMP2^{+/cKO}$ mice. Furthermore, AMD3100 treatment at early stage of fracture repair restored the callus formation in $BMP2^{+/cKO}$, indicating that the deranged CXCL12 endosteal response was corrected.

Although most of the studies report that CXCR7 represents a “decoy” receptor functioning as scavenging for CXCL12, recent studies have reported that CXCR7 may induce some signaling (reviewed in Jantunen and colleagues[46]). Furthermore, AMD3100, although largely characterized as a CXCR4 antagonist, has been shown to bind CXCR7 with allosteric agonist (reviewed in Jantunen and colleagues[46]). Unfortunately, we could not find a reliable antibody to assess the expression pattern of CXCR7 during fracture and in BMP2 mutants. The in vitro studies showed that isolated endosteal cells from $BMP2^{cKO/cKO}$ had CXCR7 and CXCR4 expression levels similar to controls, whereas CXCL12 was increased. BMP2 treatment did not affect CXCR7 or CXCR4, but did decrease CXCL12 expression levels. AMD3100 did not affect CXCR7, but did decrease CXCR4 expression levels. Studies on mice carrying a conditionally inactivated copy of CXCR4 in osteoprecursors have showed that CXCR4 regulates osteoblastic differentiation in cooperation with BMP signaling.[47] In future studies it would be interesting to evaluate the CXCL12 receptors and the intracellular signaling elicited by CXCL12 that is affected by AMD3100, as well as this intriguing bidirectional crosstalk between BMP2 and CXCL12 as well as CXCR4 and BMP signaling.

Although we are still far from unequivocally defining MSC in vivo in adult mice, some progress has been made in the identification, localization, and actions of MSCs.[48–51] It appears that MSCs exert their regenerative functions through autocrine and paracrine mechanisms acting as the seed and the soil of tissue repair. It is also becoming evident that MSCs can arise from a spectrum of bona fide progenitors that can be prospectively identified, within specific niches, by expression of novel reparative proteins in response to injury. Here we report that a population of perivascular endosteal cells begins to express BMP2 in response to the fracture injury event. Furthermore, we showed that transplanted MSCs begin to express BMP2 at the fracture endosteal site. Last, we found that BMP2 produced either by perivascular endosteal cells, transplanted MSCs, or cultured MSCs has a functional role in promoting fracture healing and osteogenesis by regulating CXCL12 temporal and spatial expression. Studies have indicated that a population of MSCs can be derived from pericytes.[52,53] In addition, it appears that pericytes are capable of promoting angiogenesis, whereas MSC are not.[54] Consistent with these reports, we hypothesize that during fracture repair perivascular cells start to express BMP2, become committed to pericytes-MSCs and therefore committed to osteogenesis while departing from their supportive role in angiogenesis (Fig. 7). Consensus regarding the origin, relationship, and fate of MSCs and pericytes remains equivocal mostly because MSCs and pericytes share several molecular markers and functions. Our studies provide novel evidence for in vitro and in vivo functional relationship between perivascular cells and MSC. Our findings may lead to the development of functional studies and identification of unique markers that would distinguish MSCs from pericytes. Beneficial effects of MSCs in facilitating fracture repair have been reported in animal models and in preliminary clinical studies.[55–59] Our studies provide evidence for a mechanism for such reparative actions through the delivery of BMP2.

The use of BMPs in fractures and in non-unions has shown promising results. There is evidence that BMPs reduce the time for fracture healing and in non-unions lead to similar results to autograft (reviewed in Ronga and colleagues[60]). However, several complications have been reported particularly in spinal surgery, mostly related to ectopic bone formation (reviewed in Ronga and colleagues[60]). Furthermore, the high costs of BMPs must be considered in the evaluation of their efficacy. Our studies have clinical impact in the treatment of non-unions or to accelerate healing in patients with comorbidities as they provide mechanistic evidence for MSC-based therapy as well as the basis for developing a pharmacological approach by using the U.S. Food and Drug Administration (FDA)-approved AMD3100 (Plerixafor).

Evidence of the coupling of angiogenesis and bone formation, specifically osteogenesis, in fracture healing exists.[61] In BMP2 haploinsufficient mice and cells, along with failure to properly heal and lack of osteogenic differentiation, high CXCL12 expression correlated with abnormal angiogenesis that was corrected by altering the CXCL12 signaling. CXCL12 and PECAM followed an apparently related expression pattern. We postulate that in the absence of BMP2, perivascular cells maintain high levels of CXCL12 that promote their supportive functions of endothelial cells, therefore uncoupling the bone/angiogenesis process by favoring angiogenesis.

Taken together, our studies show that a well-controlled regulation of BMP2 on CXCL12 expression in time, pattern, and localization is essential for fracture repair. This has far-reaching implications for our understanding of the fracture repair process and to promote healing by intervening into these mechanisms.

Supplementary Material

Refer to Web version on PubMed Central for supplementary material.

Acknowledgments

This work was supported by the National Institute of Arthritis and Musculoskeletal and Skin Diseases and the National Institute of Diabetes and Digestive and Kidney Diseases of the National Institutes of Health (R01 DK070929 to AS and F32 AR060113 to TJM). We thank the UNC Histological Research Core and the Biomedical Research Imaging Center for their technical assistance. We thank Dr. Daniel Link (Washington University) for the insightful suggestions regarding CXCL12 biology and ISH studies; Dr. Mortlock (Vanderbilt University) for providing the BMP2-LacZ reporter mice; and Dr. James Martin (Texas A&M Health Science Center) for the $BMP2^{flox/flox}$.

References

1. Burge R, Dawson-Hughes B, Solomon DH, Wong JB, King A, Tosteson A. Incidence and economic burden of osteoporosis-related fractures in the United States, 2005–2025. J Bone Miner Res. 2007; 22(3):465–75. [PubMed: 17144789]
2. Einhorn TA. Enhancement of fracture-healing. J Bone Joint Surg Am. 1995; 77(6):940–56. [PubMed: 7782368]
3. Marsh D. Concepts of fracture union, delayed union, and nonunion. Clin Orthop Relat Res. 1998; 355(Suppl):S22–30. [PubMed: 9917623]
4. Praemer, A.; Furner, S.; Rice, DP. Musculoskeletal conditions in the United States. 2. Rosemont, IL: The American Academy of Orthopaedic Surgeons; 1999.

5. Einhorn TA. The cell and molecular biology of fracture healing. Clin Orthop Relat Res. 1998; (355 Suppl):S7–21. [PubMed: 9917622]
6. Cho TJ, Gerstenfeld LC, Einhorn TA. Differential temporal expression of members of the transforming growth factor beta superfamily during murine fracture healing. J Bone Miner Res. 2002; 17(3):513–20. [PubMed: 11874242]
7. Tsuji K, Bandyopadhyay A, Harfe BD, et al. BMP2 activity, although dispensable for bone formation, is required for the initiation of fracture healing. Nat Genet. 2006; 38(12):1424–9. [PubMed: 17099713]
8. Kwong FN, Hoyland JA, Evans CH, Freemont AJ. Regional and cellular localisation of BMPs and their inhibitors' expression in human fractures. Int Orthop. 2009; 33(1):281–8. [PubMed: 19023570]
9. Kwong FN, Hoyland JA, Freemont AJ, Evans CH. Altered relative expression of BMPs and BMP inhibitors in cartilaginous areas of human fractures progressing towards nonunion. J Orthop Res. 2009; 27(6):752–7. [PubMed: 19058174]
10. Kitaori T, Ito H, Schwarz EM, et al. Stromal cell-derived factor 1/CXCR4 signaling is critical for the recruitment of mesenchymal stem cells to the fracture site during skeletal repair in a mouse model. Arthritis Rheum. 2009; 60(3):813–23. [PubMed: 19248097]
11. Lee DY, Cho TJ, Lee HR, et al. Distraction osteogenesis induces endothelial progenitor cell mobilization without inflammatory response in man. Bone. 2010; 46(3):673–9. [PubMed: 19853677]
12. Wise JK, Sumner DR, Virdi AS. Modulation of stromal cell-derived factor-1/CXC chemokine receptor 4 axis enhances rhBMP-2-induced ectopic bone formation. Tissue Eng Part A. 2012; 18(7–8):860–9. [PubMed: 22035136]
13. Dar A, Kollet O, Lapidot T. Mutual, reciprocal SDF-1/CXCR4 interactions between hematopoietic and bone marrow stromal cells regulate human stem cell migration and development in NOD/SCID chimeric mice. Exp Hematol. 2006; 34(8):967–75. [PubMed: 16863903]
14. Kumar S, Ponnazhagan S. Mobilization of bone marrow mesenchymal stem cells in vivo augments bone healing in a mouse model of segmental bone defect. Bone. 2012; 50(4):1012–8. [PubMed: 22342795]
15. Jiang Y, Bonig H, Ulyanova T, Chang K, Papayannopoulou T. On the adaptation of endosteal stem cell niche function in response to stress. Blood. 2009; 114(18):3773–82. [PubMed: 19724056]
16. Cashman J, Clark-Lewis I, Eaves A, Eaves C. Stromal-derived factor 1 inhibits the cycling of very primitive human hematopoietic cells in vitro and in NOD/SCID mice. Blood. 2002; 99(3):792–9. [PubMed: 11806978]
17. Kortesidis A, Zannettino A, Isenmann S, Shi S, Lapidot T, Gronthos S. Stromal-derived factor-1 promotes the growth, survival, and development of human bone marrow stromal stem cells. Blood. 2005; 105(10):3793–801. [PubMed: 15677562]
18. Greenbaum A, Hsu YM, Day RB, et al. CXCL12 in early mesenchymal progenitors is required for haematopoietic stem-cell maintenance. Nature. 2013; 495(7440):227–30. [PubMed: 23434756]
19. Mendez-Ferrer S, Michurina TV, Ferraro F, et al. Mesenchymal and haematopoietic stem cells form a unique bone marrow niche. Nature. 2010; 466(7308):829–34. [PubMed: 20703299]
20. Hosogane N, Huang Z, Rawlins BA, et al. Stromal derived factor-1 regulates bone morphogenetic protein 2-induced osteogenic differentiation of primary mesenchymal stem cells. Int J Biochem Cell Biol. 2010; 42(7):1132–41. [PubMed: 20362069]
21. Zhu W, Boachie-Adjei O, Rawlins BA, et al. A novel regulatory role for stromal-derived factor-1 signaling in bone morphogenic protein-2 osteogenic differentiation of mesenchymal C2C12 cells. J Biol Chem. 2007; 282(26):18676–85. [PubMed: 17439946]
22. Liu C, Weng Y, Yuan T, et al. CXCL12/CXCR4 signal axis plays an important role in mediating bone morphogenetic protein 9-induced osteogenic differentiation of mesenchymal stem cells. Int J Med Sci. 2013; 10(9):1181–92. [PubMed: 23935395]
23. Ma L, Martin JF. Generation of a Bmp2 conditional null allele. Genesis. 2005; 42(3):203–6. [PubMed: 15986484]

24. Logan M, Martin JF, Nagy A, Lobe C, Olson EN, Tabin CJ. Expression of Cre recombinase in the developing mouse limb bud driven by a Prxl enhancer. Genesis. 2002; 33(2):77–80. [PubMed: 12112875]
25. Chandler RL, Chandler KJ, McFarland KA, Mortlock DP. Bmp2 transcription in osteoblast progenitors is regulated by a distant 3′ enhancer located 156.3 kilobases from the promoter. Mol Cell Biol. 2007; 27(8):2934–51. [PubMed: 17283059]
26. Granero-Molto F, Weis JA, Miga MI, et al. Regenerative effects of transplanted mesenchymal stem cells in fracture healing. Stem Cells. 2009; 27(8):1887–98. [PubMed: 19544445]
27. Granero-Molto F, Myers TJ, Weis JA, et al. Mesenchymal stem cells expressing insulin-like growth factor-I (MSCIGF) promote fracture healing and restore new bone formation in Irs1 knockout mice: analyses of MSCIGF autocrine and paracrine regenerative effects. Stem Cells. 2011; 29(10): 1537–48. [PubMed: 21786367]
28. Weis JA, Miga MI, Granero-Molto F, Spagnoli A. A finite element inverse analysis to assess functional improvement during the fracture healing process. J Biomech. 2010; 43(3):557–62. [PubMed: 19875119]
29. Spagnoli A, O'Rear L, Chandler RL, et al. TGF-beta signaling is essential for joint morphogenesis. J Cell Biol. 2007; 177(6):1105–17. [PubMed: 17576802]
30. Balduino A, Hurtado SP, Frazao P, et al. Bone marrow subendosteal microenvironment harbours functionally distinct haemosupportive stromal cell populations. Cell Tissue Res. 2005; 319(2): 255–66. [PubMed: 15578225]
31. Balduino A, Mello-Coelho V, Wang Z, et al. Molecular signature and in vivo behavior of bone marrow endosteal and subendosteal stromal cell populations and their relevance to hematopoiesis. Exp Cell Res. 2012; 318(19):2427–37. [PubMed: 22841688]
32. Sugiyama T, Kohara H, Noda M, Nagasawa T. Maintenance of the hematopoietic stem cell pool by CXCL12-CXCR4 chemokine signaling in bone marrow stromal cell niches. Immunity. 2006; 25(6):977–88. [PubMed: 17174120]
33. Kollet O, Shivtiel S, Chen YQ, et al. HGF, SDF-1, and MMP-9 are involved in stress-induced human CD34+ stem cell recruitment to the liver. J Clin Invest. 2003; 112(2):160–9. [PubMed: 12865405]
34. Forde S, Tye BJ, Newey SE, et al. Endolyn (CD164) modulates the CXCL12-mediated migration of umbilical cord blood CD133+ cells. Blood. 2007; 109(5):1825–33. [PubMed: 17077324]
35. Omatsu Y, Sugiyama T, Kohara H, et al. The essential functions of adipo-osteogenic progenitors as the hematopoietic stem and progenitor cell niche. Immunity. 2010; 33(3):387–99. [PubMed: 20850355]
36. Grcevic D, Pejda S, Matthews BG, et al. In vivo fate mapping identifies mesenchymal progenitor cells. Stem Cells. 2012; 30(2):187–96. [PubMed: 22083974]
37. Matthews BG, Grcevic D, Wang L, et al. Analysis of alphaSMA-labeled progenitor cell commitment identifies notch signaling as an important pathway in fracture healing. J Bone Miner Res. 2014; 29(5):1283–94. [PubMed: 24190076]
38. McNulty MA, Virdi AS, Christopherson KW, Sena K, Frank RR, Sumner DR. Adult stem cell mobilization enhances intramembranous bone regeneration: a pilot study. Clin Orthop Relat Res. 2012; 470(9):2503–12. [PubMed: 22528386]
39. Yellowley C. CXCL12/CXCR4 signaling and other recruitment and homing pathways in fracture repair. Bonekey Rep. 2013 Mar 13.2:300. [PubMed: 24422056]
40. Leucht P, Temiyasathit S, Russell A, et al. CXCR4 antagonism attenuates load-induced periosteal bone formation in mice. J Orthop Res. 2013; 31(11):1828–38. [PubMed: 23881789]
41. Toupadakis CA, Wong A, Genetos DC, et al. Long-term administration of AMD3100, an antagonist of SDF-1/CXCR4 signaling, alters fracture repair. J Orthop Res. 2012; 30(11):1853–9. [PubMed: 22592891]
42. Colnot C. Skeletal cell fate decisions within periosteum and bone marrow during bone regeneration. J Bone Miner Res. 2009; 24(2):274–82. [PubMed: 18847330]
43. Colnot C, Huang S, Helms J. Analyzing the cellular contribution of bone marrow to fracture healing using bone marrow transplantation in mice. Biochem Biophys Res Commun. 2006; 350(3):557–61. [PubMed: 17022937]

44. Colnot C, Zhang X, Knothe Tate ML. Current insights on the regenerative potential of the periosteum: molecular, cellular, and endogenous engineering approaches. J Orthop Res. 2012; 30(12):1869–78. [PubMed: 22778049]
45. Ozaki A, Tsunoda M, Kinoshita S, Saura R. Role of fracture hematoma and periosteum during fracture healing in rats: interaction of fracture hematoma and the periosteum in the initial step of the healing process. J Orthop Sci. 2000; 5(1):64–70. [PubMed: 10664441]
46. Jantunen E, Varmavuo V. Plerixafor for mobilization of blood stem cells in autologous transplantation: an update. Expert Opin Biol Ther. 2014; 14(6):851–61. [PubMed: 24673120]
47. Zhu W, Liang G, Huang Z, Doty SB, Boskey AL. Conditional inactivation of the CXCR4 receptor in osteoprecursors reduces postnatal bone formation due to impaired osteoblast development. J Biol Chem. 2011; 286(30):26794–805. [PubMed: 21636574]
48. Bianco P, Robey PG, Simmons PJ. Mesenchymal stem cells: revisiting history, concepts, and assays. Cell Stem Cell. 2008; 2(4):313–9. [PubMed: 18397751]
49. Bianco P, Cao X, Frenette PS, et al. The meaning, the sense and the significance: translating the science of mesenchymal stem cells into medicine. Nat Med. 2013; 19(1):35–42. [PubMed: 23296015]
50. Worthley DL, Churchill M, Compton JT, et al. Gremlin 1 identifies a skeletal stem cell with bone, cartilage, and reticular stromal potential. Cell. 2015; 160(1–2):269–84. [PubMed: 25594183]
51. Zhou BO, Yue R, Murphy MM, Peyer JG, Morrison SJ. Leptin-receptor-expressing mesenchymal stromal cells represent the main source of bone formed by adult bone marrow. Cell Stem Cell. 2014; 15(2):154–68. [PubMed: 24953181]
52. Crisan M, Yap S, Casteilla L, et al. A perivascular origin for mesenchymal stem cells in multiple human organs. Cell Stem Cell. 2008; 3(3):301–13. [PubMed: 18786417]
53. Feng J, Mantesso A, De Bari C, Nishiyama A, Sharpe PT. Dual origin of mesenchymal stem cells contributing to organ growth and repair. Proc Natl Acad Sci USA. 2011; 108(16):6503–8. [PubMed: 21464310]
54. Blocki A, Wang Y, Koch M, et al. Not all MSCs can act as pericytes: functional in vitro assays to distinguish pericytes from other mesenchymal stem cells in angiogenesis. Stem Cells Dev. 2013; 22(17):2347–55. [PubMed: 23600480]
55. Hernigou P, Poignard A, Beaujean F, Rouard H. Percutaneous autologous bone-marrow grafting for nonunions. Influence of the number and concentration of progenitor cells. J Bone Joint Surg. 2005; 87(7):1430–7. [PubMed: 15995108]
56. Kon E, Muraglia A, Corsi A, et al. Autologous bone marrow stromal cells loaded onto porous hydroxyapatite ceramic accelerate bone repair in critical-size defects of sheep long bones. J Biomed Mater Res. 2000; 49(3):328–37. [PubMed: 10602065]
57. Marcacci M, Kon E, Moukhachev V, et al. Stem cells associated with macroporous bioceramics for long bone repair: 6- to 7-year outcome of a pilot clinical study. Tissue Eng. 2007; 13(5):947–55. [PubMed: 17484701]
58. Quarto R, Mastrogiacomo M, Cancedda R, et al. Repair of large bone defects with the use of autologous bone marrow stromal cells. N Engl J Med. 2001; 344(5):385–6. [PubMed: 11195802]
59. Watson L, Elliman SJ, Coleman CM. From isolation to implantation: a concise review of mesenchymal stem cell therapy in bone fracture repair. Stem Cell Res Ther. 2014; 5(2):51. [PubMed: 25099622]
60. Ronga M, Fagetti A, Canton G, Paiusco E, Surace MF, Cherubino P. Clinical applications of growth factors in bone injuries: experience with BMPs. Injury. 2013; 44(Suppl 1):S34–39. [PubMed: 23351868]
61. Maes C, Kobayashi T, Selig MK, et al. Osteoblast precursors, but not mature osteoblasts, move into developing and fractured bones along with invading blood vessels. Dev Cell. 2010; 19(2):b329–44.

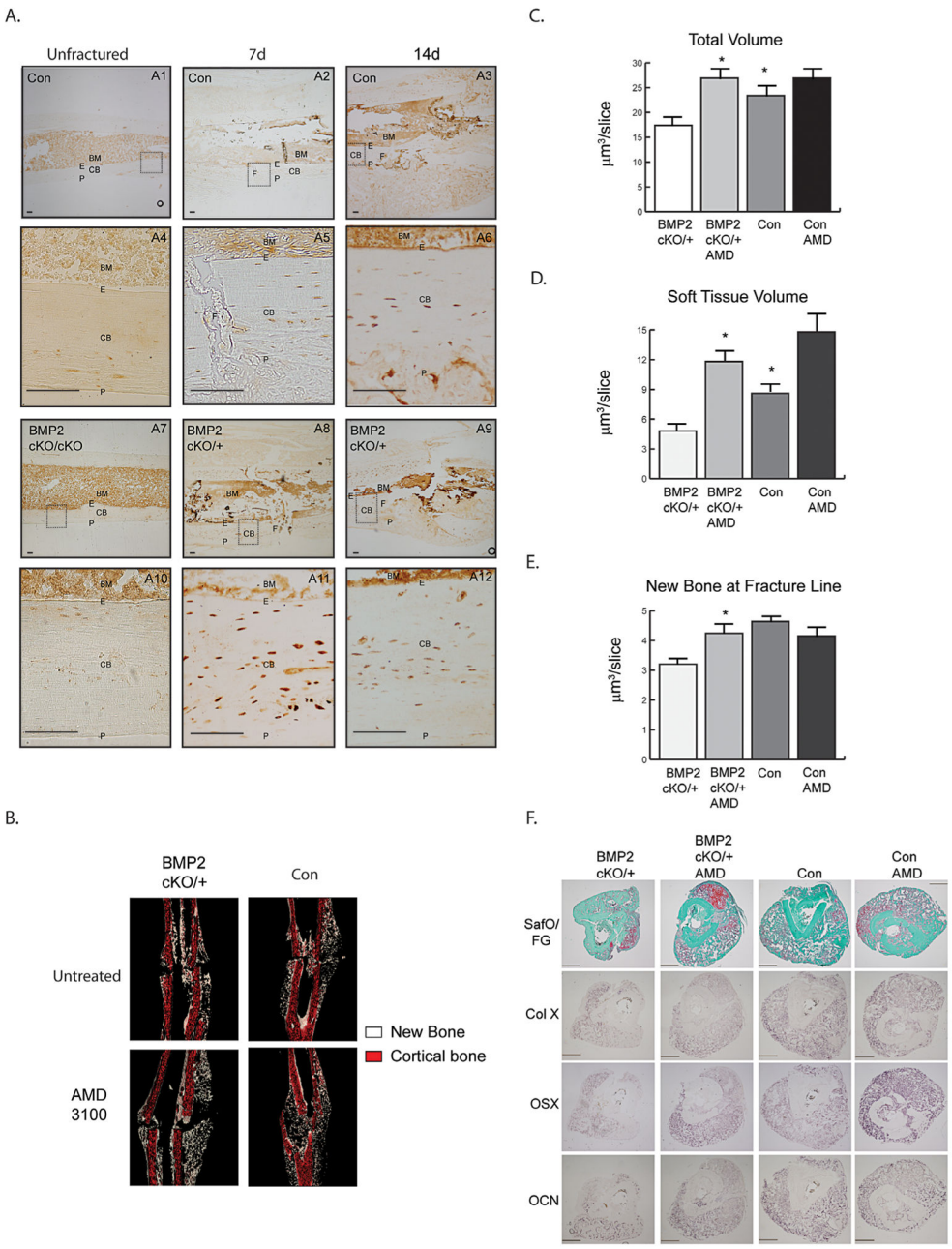

Fig. 1.

CXCL12 expression and BMP2-dependent function in fracture healing. (*A*) Representative images of immunohistochemical staining for CXCL12 (brown) from unfractured (A1, A4, A7, A10), 7 days postfracture (A2, A5, A8, A11), and 14 days postfracture (A3, A6, A9, A12), control (A1–A6) and BMP2$^{cKO/+}$ (A7–A12) mice along and underneath the endosteum adjacent to the fracture line. Dotted squares in A1, A2, A3, A7, A8, and A9 indicate areas magnified, respectively, in A4, A5, A6, A10, A11, and A12. Scale bars =100 µm. (*B*) Representative coronal images of new (white) and cortical (red) bone from three-dimensional reconstruction of 14-day postfracture samples. Shown is a 12 µm-thick coronal

section oriented to show the facture line and callus, 14 days after fracture. Volumes of (*C*) total callus and (*D*) soft tissue normalized to the number of slices (mm^3/slice) comprising the callus (see Materials and Methods section for more details). (*E*) Volume of new bone normalized to the number of slices (mm^3/slice) from the fracture line (see Materials and Methods section for more details). (*F*) Representative histological staining for safranin O/Fast green (SafO/FG), or in situ hybridization for collagen X, OSX, OCN, and collagen I. Scale bars =500 μm. Data are expressed as mean ± SE. Control (con), n =15; $BMP2^{cKO/+}$, n =6; $BMP2^{cKO/+}$+AMD and Con +AMD, n =7. *p <0.05 compared to $BMP2^{cKO/+}$ by one-way ANOVA and Sidak's multiple comparison test. BM =bone marrow; E =endosteum; CB =cortical bone; P =periosteum; F =fracture line; OSX =osterix; OCN =osteocalcin.

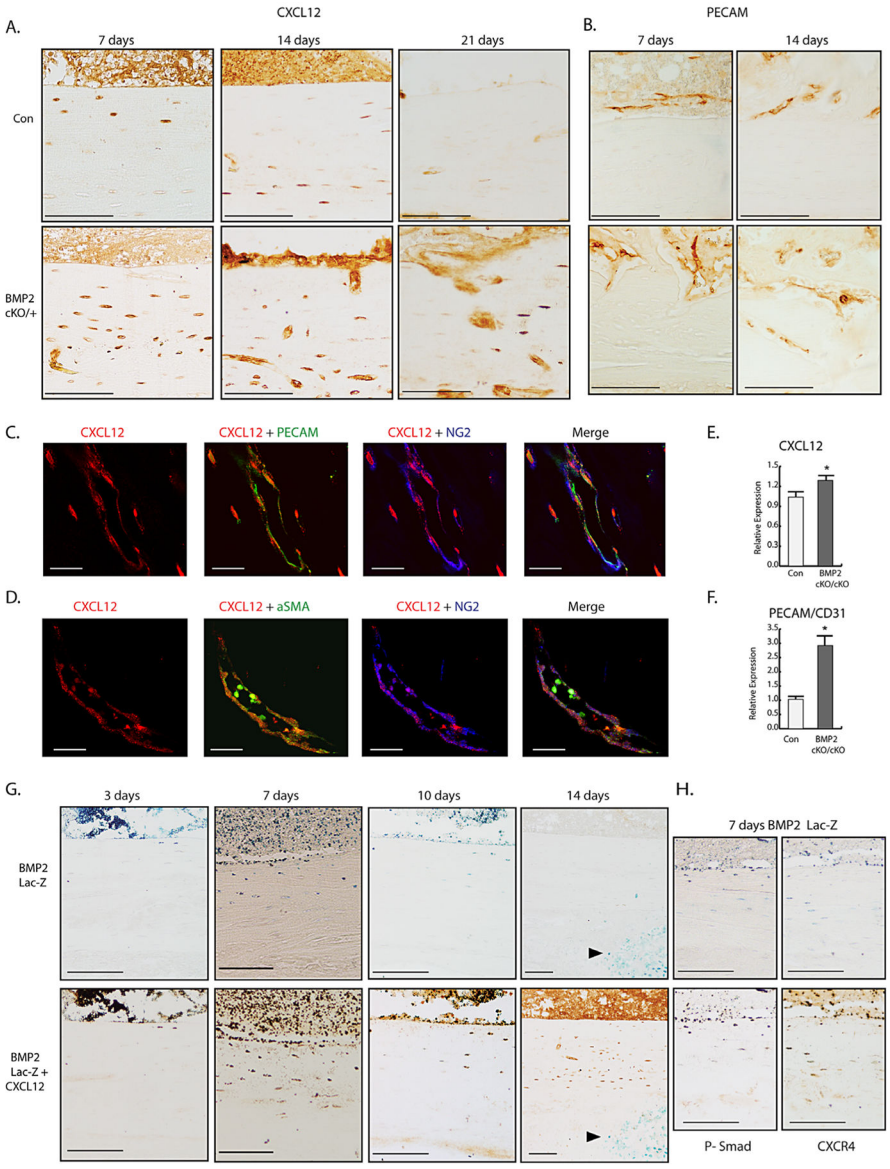

Fig. 2.

Identification of CXCL12^{+}-BMP2^{+} endosteal-perivascular cells in response to fracture and aberrant expression pattern in BMP2$^{cKO/+}$. (*A*) Representative CXCL12 IHC (brown) at 7, 14, or 21 days postfracture in control (con) and BMP2$^{cKO/+}$ samples. Scale bars for 7 and 14 day =100 μm; Scale bars for 21 day =50 μm. (*B*) Representative IHC for PECAM 7 and 14 days postfracture in control and BMP2$^{cKO/+}$ samples. Scale bars =100 μm. (*C*) Cortical bone vasculature from frozen sections of fractured BMP2$^{cKO/+}$ samples stained with antibodies against CXCL12 (red), PECAM/CD31 (green), and NG2 (blue) and then merged to show coexpression of CXCL12 and NG2 (pink). Scale bars =20 μm. (*D*) Cortical bone vasculature from frozen sections of fractured BMP2$^{cKO/+}$ samples stained with antibodies against CXCL12 (red), α-SMA (green), and NG2 (blue) and then merged to show coexpression of CXCL12 and α-SMA (yellow). Scale bars =20 μm. mRNA expression levels by qRT-PCR of CXCL12 (*E*) or PECAM/CD31 (*F*) in control or BMP2$^{cKO/cKO}$ endosteal cells. (*G*, *H*) Top

panels depict representative LacZ stained sections from BMP2-LacZ reporter mice 3, 7, 10, and 14 days after fracture as imaging reporter for BMP2 expression (blue); sections were then subjected to CXCL12 (bottom, *G*), phospho-SMAD1/5/8 (bottom, left, *H*), and CXCR4 (bottom right, *H*) IHC over the fracture healing time course. Scale bars =100 μm. Data are reported as mean ± SE of triplicate repeats from 3 separate samples normalized to control. *$p < 0.05$ compared to control by unpaired two-tailed *t* test. For all pictures, endosteal surface is facing the top of the images.

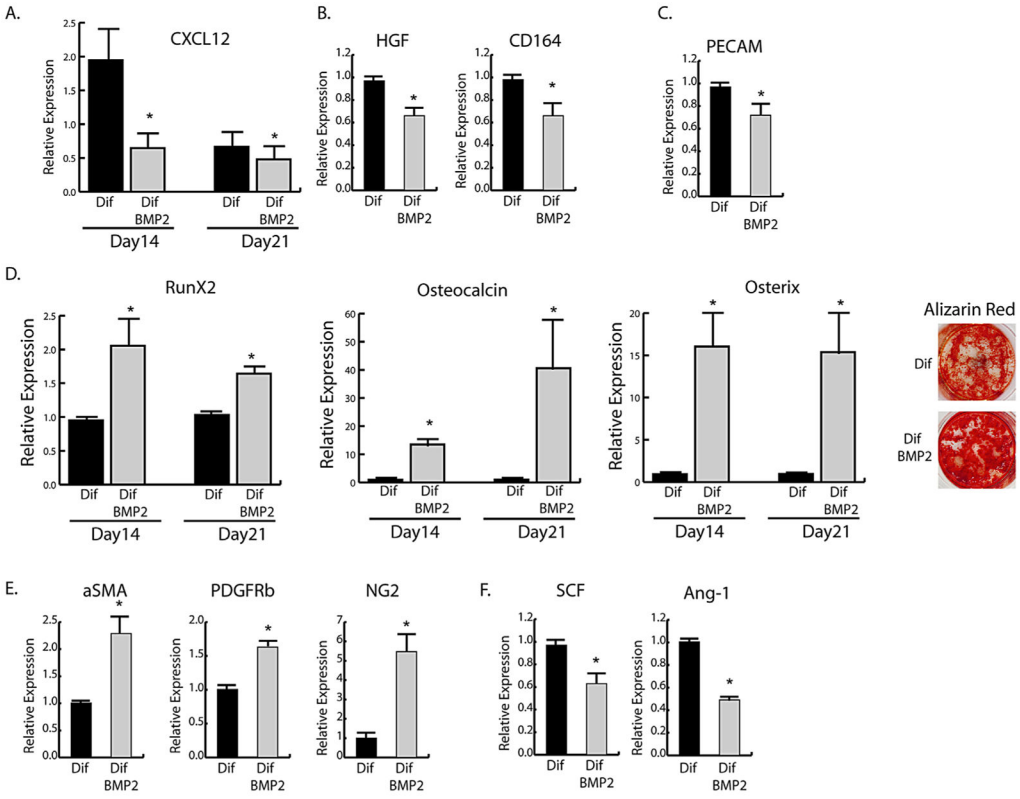

Fig. 3.

BMP2 effects on isolated endosteal cells. mRNA expression levels by qRT-PCR of (*A*) CXCL12, (*B*) day 14 CXCL12 supporting genes, (*C*) day 21 PECAM, (*D*) osteogenic markers and day 21 Alizarin red staining, (*E*) day 21 pericyte markers and (*F*) day 14 endosteal niche supporting genes from control endosteal cells in differentiating media with (Dif BMP2) or without (Dif) 100 ng/mL rhBMP2. Data are expressed as mean ± SE of triplicate repeats from 3 separate samples normalized to day 0 control (*A*) or Dif (*B*–*F*). *$p < 0.05$ compared to Dif by unpaired two-tailed *t* test.

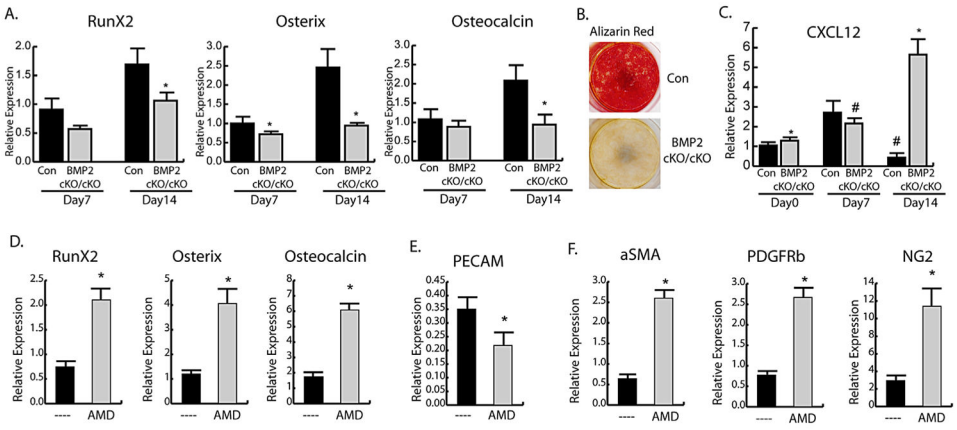

Fig. 4.

BMP-2-dependent effects of CXCL12 in controlling the osteogenic fate of endosteal cells. (*A*) mRNA expression levels by qRT-PCR of osteogenic markers during differentiation of control (Con) or BMP2$^{cKO/cKO}$ endosteal cells. (*B*) Alizarin red staining after 21 days differentiation demonstrating lack of mineralization and osteoblastic differentiation of BMP2$^{cKO/cKO}$ endosteal cells. (*C*) mRNA expression of CXCL12 over time in control and BMP2$^{cKO/cKO}$ endosteal cells. mRNA expression of (*D*) osteogenic markers or (*E*) PECAM and (*F*) pericyte markers after 14 days of BMP2$^{cKO/cKO}$ endosteal cells under differentiation conditions with or without 400 μM AMD3100 every 3 days beginning on day 7 through day 14. Data are reported as mean ± SE of triplicate repeats from 3 separate samples for *A*–*C* or triplicates repeats of quadruplicate samples for *D*–*F* normalized to day 0 control. *p <0.05 compared to Con by unpaired two-tailed t test. #p <0.05 compared to Con day 0 by one-way ANOVA and Sidak's multiple comparison test.

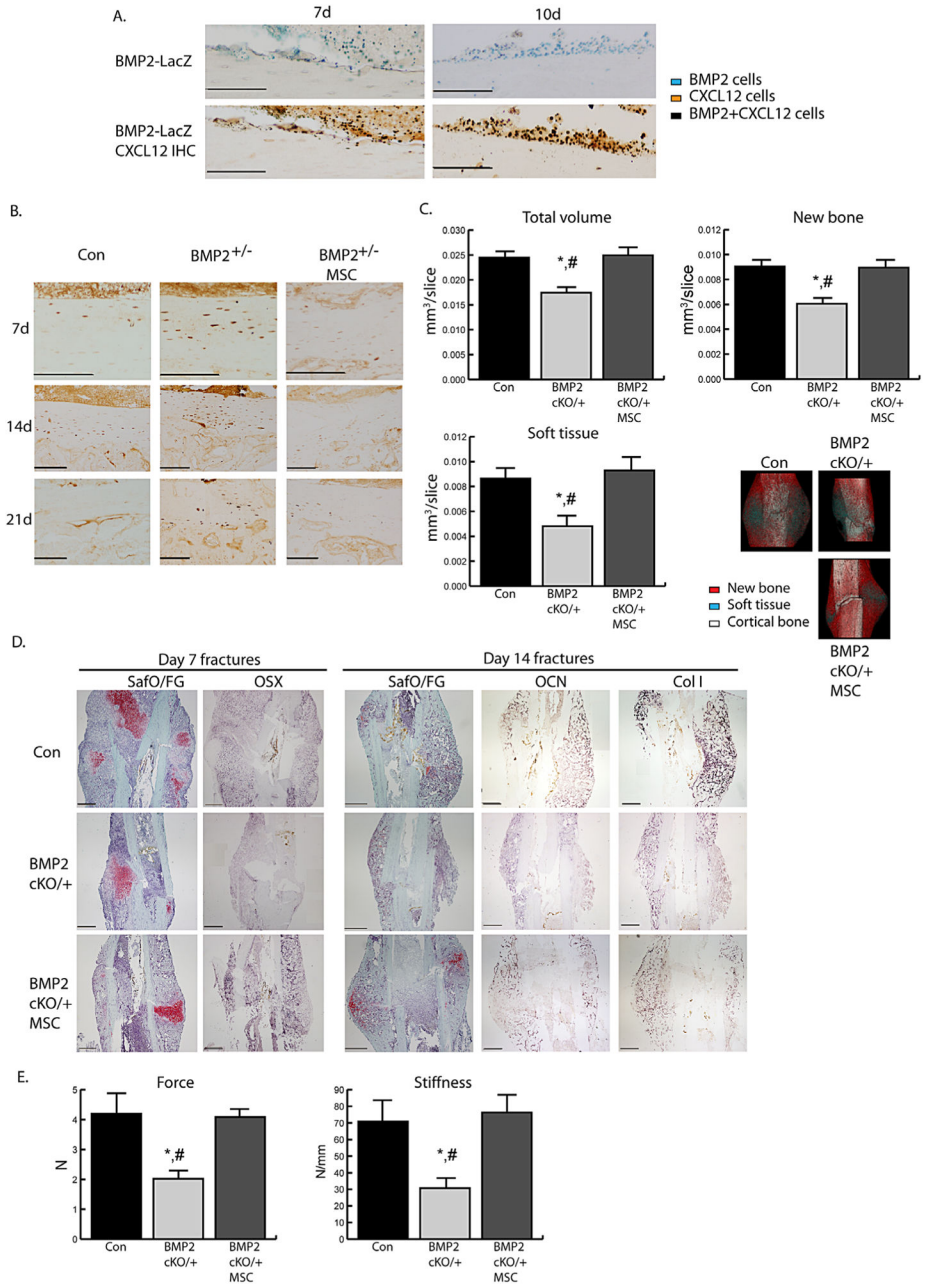

Fig. 5.

MSC transplant can rescue CXCL12 regulation and fracture healing in BMP2$^{cKO/+}$ mice. (*A*) Representative LacZ staining (top) at 7 days and 10 days postfracture of control mice transplanted with MSCs from BMP2-LacZ reporter mice (blue) followed by CXCL12 IHC (bottom, brown) of the endosteum immediately adjacent to the fracture line. Black represents cells that are BMP2^{+} (Lac-Z) and CXCL12^{+} double positive. Scale bars =100 μm. (*B*) Representative CXCL12 IHC at 7, 14, and 21 days postfracture in control (Con), BMP2$^{cKO/+}$, and BMP2$^{cKO/+}$ transplanted with MSC specimens. Scale bars for 7 and 14 day =100 μm; scale bars for 21 day =50 μm. (*C*) Volumes of total callus, new bone, and soft

tissue normalized to the number of slices (mm^3/slice) comprising the callus (see Materials and Methods section for more details). Also shown are representative three-dimensional reconstructions of μCT images consisting of new bone (red), soft tissue (turquoise), and cortical bone (white). Con, n =15; $BMP2^{cKO/+}$, n =6; $BMP2^{cKO/+}$+MSCs, n =9. (*D*) Representative histological staining for safranin O/Fast green (SafO/FG), or ISH for day 7 osterix (OSX), and day 14 osteocalcin (OCN) and collagen I. Scale bars =500 μm. (*E*) Results for distraction-to-failure biomechanical test for ultimate force and callus stiffness at 14 days postfracture. n =9. All data are mean ± SE. *p <0.05 compared to Con and #p <0.05 compared to $BMP2^{cKO/+}$ with MSCs by one-way ANOVA and Sidak's multiple comparison test. For all pictures, endosteal surface is facing the top of the images.

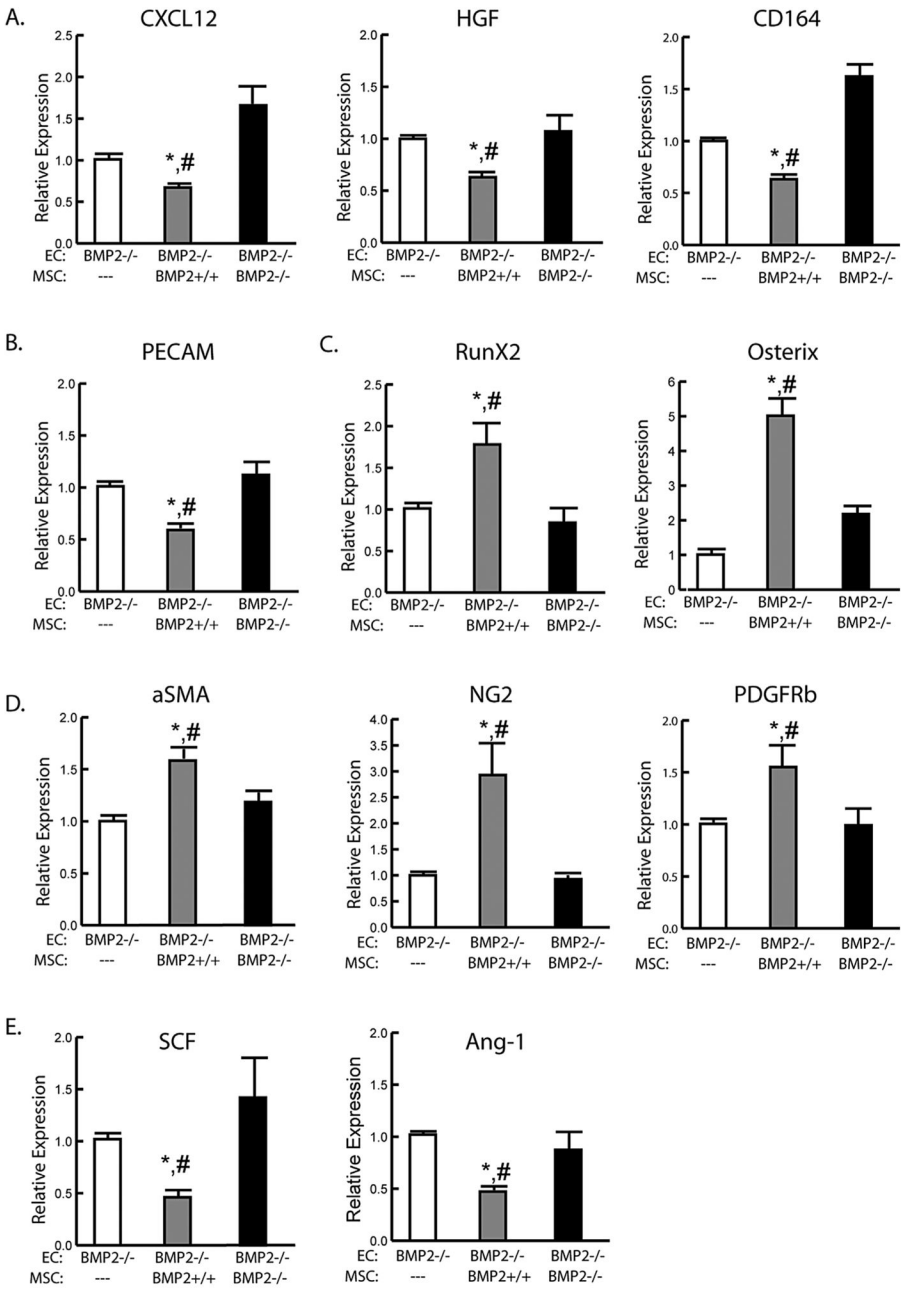

Fig. 6.

MSC-derived BMP2 can rescue CXCL12 regulation and differentiation in endosteal cells. mRNA expression levels by qRT-PCR of (*A*) CXCL12 and supporting genes, (*B*) PECAM, (*C*) osteogenic markers, (*D*) pericyte markers, and (*E*) endosteal niche supporting genes from $BMP2^{cKO/cKO}$ endosteal cells cocultured with no MSCs (---), control MSCs (+/+) or BMP2 cKO MSCs (−/−) after 14 days in osteogenic differentiation conditions. Data are reported as mean ± SE of triplicate repeats from 3 separate samples normalized to no MSCs controls. *p <0.05 compared to MSCs (---) and #p <0.05 compared to MSCs(−/−) by one-way ANOVA and Sidak's multiple comparison test.

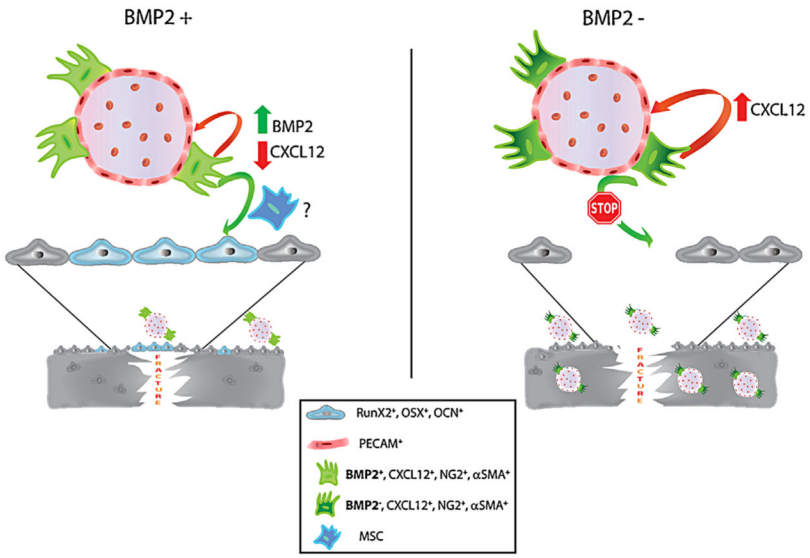

Fig. 7.

Model describing the functional role of BMP2 in fracture repair. Following fracture, a CXCL12+/BMP2+ endosteal-perivascular cell population is recruited along the endosteum. A timely increase of BMP2 leads to downregulation of CXCL12, an event which is essential for guiding the fate of the perivascular cells into pericytes that conceivably through MSCs are committed to osteoblasts integrating into the newly forming bones. In the absence of BMP2, such tight regulation of CXCL12 is lost and the $CXCL12^{+}/BMP2^{-}$ endosteal-perivascular cells become committed to their endothelial-supportive role, leading to abnormal angiogenesis and impaired fracture healing.